

High-resolution studies of collision-induced population grating resonances in optical four-wave mixing in sodium vapor

L. J. Rothberg* and N. Bloembergen

Division of Applied Sciences, Harvard University, Cambridge, Massachusetts 02138

(Received 6 July 1984)

Optical four-wave mixing resonances in sodium vapor induced by collisions with inert buffer gases (He, Ar, Xe, N₂) are characterized at high resolution (< 5 MHz) using lasers tuned near the *D* lines of Na. These resonances are interpreted in terms of coherent scattering from a population grating established by collisional absorption of the incident radiation. The roles of homogeneous and inhomogeneous contributions to the resonance line shapes are clarified. The line shapes exhibit structure sharper than the predicted linewidth, that characteristic of the 3*P*-to-3*S* transition rate. We show that this is caused by collision-induced optical pumping which introduces the ground-state lifetime into the grating relaxation physics. These long-lived gratings are exemplified dramatically by experiments in the presence of N₂ which collisionally quenches the Na 3*P* states. Similar results are obtained in Xe where it is argued that excimer formation with the 3*P* states plays a role in the population dynamics. Model calculations of the effects of sodium level degeneracy on the grating dynamics are presented to support these conclusions. Finally we present data illustrating interference between the collision-induced population grating resonances detailed here and collision-induced coherent Raman resonances between Zeeman sublevels of the ground state.

I. INTRODUCTION

Experimental observations of several types of collision-induced four-wave mixing have been reported.¹ These have been of value in elucidating the role of damping in nonlinear quantum-mechanical phenomena and in the study of atomic collisions. The role of collisions is to dephase quantum-mechanical amplitudes contributing to the four-wave mixing process which would otherwise destructively interfere. The resulting "extra" four-wave mixing resonances are characterized by intensities which increase with pressure.

A theoretical description of these resonances has been made using both semiclassical^{2,3} and quantum-mechanical^{4,5} pictures of the atom-radiation system. General expressions for the third-order susceptibility $\chi^{(3)}$ governing four-wave mixing have been derived using perturbation expansions of the density matrix in the frequency domain² and in the time domain.⁵ For comparison with the experimental results cited above, model calculations of the resonant terms in $\chi^{(3)}$ for two- and three-level systems are used. In all of the calculations to this point, collisions are incorporated in an essentially phenomenological manner and the semiclassical treatments are restricted to the impact approximation for this reason.

The correct prescription for applying time-dependent perturbation theory to the calculation of $\chi^{(3)}$ involves an iterative solution of the Liouville equation⁶ for the density matrix and introducing appropriate damping factors at each level of the calculation.² Successive perturbation of the density matrix by each incident laser field describes the superposition of material states induced by the fields which can reradiate coherently. This sequential application of laser fields suggests a picture of the four-wave mixing process as the coherent scattering of the third ap-

plied field from a grating created by the first two. This grating is a periodic spatial and/or temporal modulation of coherences (off-diagonal density-matrix elements ρ_{ij}) and/or populations (diagonal density-matrix elements ρ_{ii}). In this paper we focus on the degenerate frequency population grating resonances. In an earlier paper collision-induced coherences ρ_{ij} which give rise to Raman-type resonances have been discussed in detail.⁷ It was shown how polarization selection rules could be used to distinguish between the two effects.

Physically, the origin of coherently modulated population can be understood in terms of interference between the incident laser fields. The total intensity in the interaction region due to incident fields $\vec{E}(\omega_1)$ and $\vec{E}(\omega_2)$ is given by

$$\mathcal{I}_{\text{tot}} \propto \frac{E_1^2}{2} + \frac{E_2^2}{2} - E_1 E_2 \cos[(\omega_1 - \omega_2)t + (\vec{k}_1 - \vec{k}_2) \cdot \vec{r} + (\phi_1 - \phi_2)], \quad (1)$$

where $E_i, \omega_i, \vec{k}_i, \phi_i$ are the incident field amplitudes, frequencies, wave vectors and phases, respectively. The last term of (1) is modulated in space due to small angles between the incident beams and in time when there is a frequency mismatch between $\vec{E}(\omega_1)$ and $\vec{E}(\omega_2)$.

The intensity modulation can be translated by absorption into a spatial and temporal modulation of excited- and ground-state populations. These excited-state population "excesses" and ground-state population "holes" appear as an index modulation and a third incident light

beam can scatter coherently from this transient diffraction grating to produce the four-wave mixing signal at issue. With nonresonant radiation these coherent modulations occur only in the presence of collisions which allow absorption of radiation to couple material levels. This real-time holographic process is therefore pressure induced.

The grating picture enables us to understand several important features of population grating resonances in two-level systems. Generalizations to realistic multilevel systems with spatial angular momentum degeneracy will be discussed later. For the two-level system, the following deductions can be made.

(1) The population grating should be most intense when it is stationary in time and will therefore be resonant for $\omega_1 = \omega_2$ (degenerate frequencies).

(2) The spectral width of the resonance will reflect the rate at which holes are filled by the relaxation of the excesses, $(\pi T_1)^{-1}$. Put another way, the grating can only follow a modulation which is slow compared to the system's longitudinal relaxation time.

(3) Since the resonance depends only on population modulation, pure collisional dephasing will not affect the population relaxation rate and the resonance should not be pressure broadened except by quenching collisions.

(4) The spatial modulation of the grating can be destroyed if the atoms are free to move. This statement is equivalent to the statement that the resonance is susceptible to residual Doppler broadening.

Many authors have reported population grating resonances in four-wave mixing.⁸⁻¹⁰ These have been used to measure dye relaxation times in solution,⁸ properties of velocity changing collisions in atomic vapors,⁹ and excitation transport in solids¹⁰ to select a few examples. Extensive theoretical work on the secular terms which describe these resonances^{8,11} has aided in the interpretation of these experiments and others.

The collision-induced analogs of these resonances have been detailed in several previous papers which report the results of relatively low-resolution experiments (> 100 MHz).¹² These studies verified that collision-induced four-wave mixing resonances in sodium do occur at $\omega_1 \approx \omega_2$ and that these are not pressure broadened by inert buffer gases. However, predictions about the linewidths of these resonances could not be verified without higher-resolution experiments. The current paper presents results of high-resolution (< 5 MHz) studies of pressure-induced population grating resonances. These are separated from spectrally overlapping collision-induced coherent anti-Stokes Raman spectroscopy (CARS) and coherent Stokes Raman spectroscopy (CSRS) resonances between Zeeman sublevels of the ground state⁷ by exploiting the selection rules for the $3S \rightarrow 3P$ transition in sodium. It is demonstrated that the predictions of a simple two-level model are not sufficient to explain the four-wave mixing line shapes and that the degeneracy of the sodium levels must be considered. Results in the presence of He, Ar, Xe, and mixtures with N_2 and/or Cs are set forth and explained. Finally we report interference effects between the Zeeman and population coherences when both are allowed by the incident field configuration.

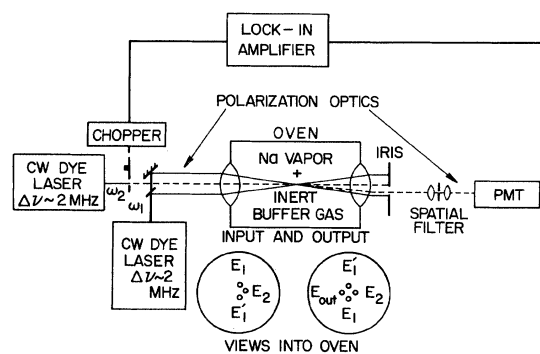


FIG. 1. Schematic of experimental apparatus for four-wave mixing.

II. EXPERIMENTAL

Figure 1 is a block diagram of the experimental arrangement which has been described in greater detail in another paper.⁷ A 6-W cw argon ion laser (Spectra Physics 171-19) pumps two frequency stabilized single mode dye lasers (CR 599-21) with rms linewidths of about 2 MHz. The first dye laser with ω_1 is split into two beams which propagate parallel separated by 2 to 3 mm. The second laser with ω_2 propagates parallel to these so that the beams are at the vertices of an isosceles right triangle as in Fig. 1. These beams are then focussed by a 5 cm lens to a common region. The resulting phase matching geometry¹³ has the advantages that the matching is constant over a wide tuning range and that completely degenerate four-wave mixing can be easily studied with only spatial discrimination. The output $2\omega_1 - \omega_2$ is at the fourth corner of the square whose other three vertices are formed by the transmitted incident beams.

The sodium oven is operated at sodium densities around $10^{13} - 10^{14}/\text{cm}^3$ with added buffer-gas pressures (He, Ar, or Xe) up to three atmospheres. The lasers are tuned approximately 30 GHz (1 cm^{-1}) below the $D_1(3^2S_{1/2} - 3^2P_{1/2})$ line of sodium, a value large compared to the Doppler width ($\Delta\nu_{\text{Dopp}} \approx 2$ GHz), to the Rabi frequency ($\nu_R \approx 10 - 100$ MHz) and to the collisional width T_2^{-1} [full width at half maximum (FWHM) ≈ 11 MHz/Torr He]. At this detuning no velocity group is preferred, one photon saturation effects are negligible and only a small amount of collisionally assisted absorption occurs. The impact approximation, however, remains valid as the detuning is much less than the inverse collision time.

The polarizations of the beams are linear and parallel for the data of Sec. III which is strictly confined to population grating resonances. In Sec. IV more complex polarization combinations are used and will be described in that section.

III. RESULTS AND DISCUSSION OF COLLISION-INDUCED POPULATION GRATING RESONANCES

We intersperse the results of model calculations with the experimental data for comparison and insight. The

susceptibility corresponding to the population grating resonances is proportional to the population modulation $(\rho_{nn}^{(2)} - \rho_{gg}^{(2)})(\omega_1 - \omega_2)$, where $|g\rangle$ and $|n\rangle$ denote ground and excited state, respectively. The four-wave mixing in-

intensities vary as the squared modulus of this quantity. The frequency domain equations for the l th-order perturbative corrections $\rho^{(l)}$ to the diagonal elements of the density matrix ρ are

$$-i(\omega_1 - \omega_2)\rho_{kk}^{(l)} = \sum_m W_{mk}\rho_{kk}^{(l)} - \sum W_{km}\rho_{kk}^{(l)} - (i/\hbar)[\mathcal{H}_{\text{coh}}, \rho^{(l-1)}]_{kk} \quad (2)$$

as given by Bloembergen and Shen.⁶ The brackets are commutators, the $W_{i \rightarrow j}$ denote population transfer rates between $|i\rangle$ and $|j\rangle$, and \mathcal{H}_{coh} is the perturbation Hamiltonian for the applied fields.

A. The two-level system

The original calculations of the population grating $\rho_{nn}^{(2)} - \rho_{gg}^{(2)}$ in a two-level system^{8,12} are reproduced here to establish a notation and a basis for further modeling. For the two-level system sketched in Fig. 2(a), Eqs. (2) can be written

$$\begin{pmatrix} -i\delta + W_{gn} & -W_{ng} \\ -W_{gn} & -i\delta + W_{ng} \end{pmatrix} \begin{pmatrix} \rho_{gg}^{(2)} \\ \rho_{nn}^{(2)} \end{pmatrix} = \begin{pmatrix} A \\ -A \end{pmatrix}, \quad (3)$$

where we have used the simplifying notation that $\delta = \omega_1 - \omega_2$ is the detuning from the difference frequency resonance. W_{gn} and W_{ng} are spontaneous population transfer rates and

$$A = (i/\hbar)[\mathcal{H}_{\text{coh}}, (\omega - \omega_{ng} + i\Gamma_{ng})^{-1}[\mathcal{H}_{\text{coh}}, \rho^{(0)}]]$$

describes the field induced population transfer where Γ_{ng} is the damping width of the $|n\rangle$ to $|g\rangle$ transition, equal to T_2^{-1} in the two-level case. Using the conventional definition that $T_1^{-1} = W_{gn} + W_{ng}$ gives

$$\begin{aligned} \chi^{(3)} \alpha \rho_{nn}^{(2)} - \rho_{gg}^{(2)} &= \frac{-2iA}{\delta + 1/T_1} \\ &= \frac{\mu_{gn}\mu_{ng}E_1E_2^*(\rho_{nn}^{(0)} - \rho_{gg}^{(0)})(\delta + 2i\Gamma_{ng})}{2\hbar^2(\delta + i/T_1)(\omega_{ng} - \omega_2 + i\Gamma_{ng})(\omega_1 - \omega_{ng} + i\Gamma_{ng})}. \end{aligned} \quad (4)$$

The value of A has been calculated explicitly using the analog to Eq. (2) for the off-diagonal elements of the density matrix, where μ_{ij} are dipole matrix elements and the ω_{ij} are transition frequencies of the two-level atom. E_i is the complex shorthand for the electric field,

$$E_i = \mathcal{E}_i e^{i(\vec{k}_i \cdot \vec{r} - \omega t)}. \quad (5)$$

Equation (4) bears out the qualitative features of these resonances put forth in the introduction. The term $E_1E_2^*$ is the complex notation equivalent of the final term in Eq. (1), which exhibits the spatial and temporal population modulation. The denominator $(\delta + i/T_1)$ embodies the resonance at $\omega_1 = \omega_2$. The full width at half maximum of this difference frequency resonance is $\pi/T_1 = 20$ MHz for the sodium D lines. We point out that this differs from the absorption resonance whose width is well known to be $\pi/T_2 = 10$ MHz. Physically, this is because the populations and coherences relax at different rates as expressed by the relation that $2T_2^{-1} = T_1^{-1}$ in the absence of pure dephasing. The four-wave mixing linewidths are only sensitive to the *populations* since the grating disappears when the excesses fill the holes. They are therefore unaffected by inert buffer gases which pressure broaden the absorptions according to

$$2T_2^{-1} = T_1^{-1} + \beta p, \quad (6)$$

where p is the buffer-gas pressure and β a proportionality constant. (The sodium pressure is assumed to be small.)

The term with $\Gamma_{ng} = T_2^{-1}$ in the numerator of (4) contains the collision-induced nature of the resonances. When $p = 0$ the expression $\delta + 2i\Gamma_{ng}$ cancels with the resonant denominator $\delta + iT_1^{-1}$ leaving no resonance. In the full 48 term expression for $\chi^{(3)}$ this corresponds to a cancellation of two terms,² a destructive interference between four-wave mixing amplitudes. At high pressures (typically $p \geq 10$ Torr) we get $\beta p \gg T_1^{-1}$, a nonlinear susceptibility proportional to pressure, and a four-wave mixing intensity proportional to p^2 . The cancellation between quantum-mechanical amplitudes is destroyed by collisional dephasing. Low-resolution work¹² has verified this pressure dependence quantitatively.

The original motivation for higher-resolution studies of these resonances was to verify the predicted linewidths. Figure 3 plots the observed linewidth as a function of added buffer-gas pressure for the population grating resonances. The reason for some of the large width at low pressure is that for simplicity we had omitted the Doppler broadening terms which should appear in Eq. (4).¹⁴ Since the one-photon Doppler widths (≤ 2 GHz) can be neglected compared to the detunings from the $|g\rangle$ to $|n\rangle$ transition (≥ 20 GHz) (see Sec. II) it is approximately correct

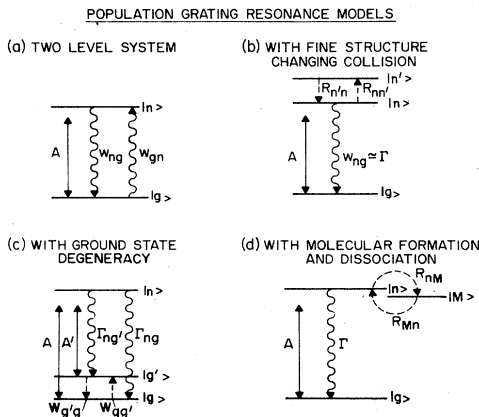


FIG. 2. Population grating resonance models.

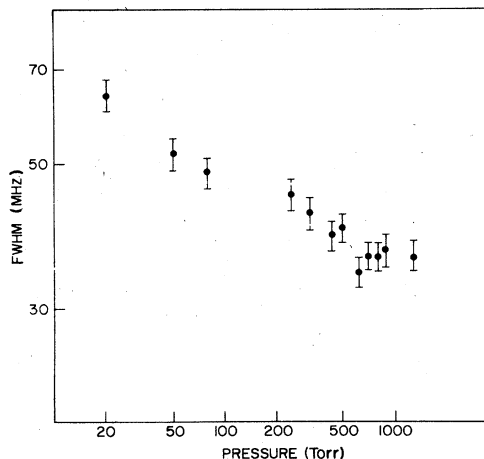


FIG. 3. Population grating resonance linewidths (FWHM) as a function of He pressure, on a double-logarithmic scale.

to add $(\vec{k}_1 - \vec{k}_2) \cdot \vec{v}$ to the terms $(\delta + iT_1^{-1})$ and $(\delta + 2i\Gamma_{ng})$ to amend Eq. (4). These widths are approximately 50–100 MHz in our experimental geometry. As mentioned in Sec. I, these corrections can be interpreted physically as describing the decay of the population modulation in space due to the atomic motion. The reason, then, for the decrease of the resonance width with pressure is that velocity changing collisions with buffer-gas atoms constrain the grating and prevent its washout. This is an appealing physical way to understand this collisional narrowing of the Doppler width, first predicted¹⁵ and observed¹⁶ by Dicke. We have published a separate paper on using the collision-induced resonance line shapes to learn about properties of velocity changing collisions.¹⁷ At the highest pressures in Fig. 3, the Doppler width has completely narrowed and the linewidths remain considerably greater than 20 MHz. No power broadening or broadening with sodium density is observed and we know independently⁷ that the instrumental width cannot explain this discrepancy.

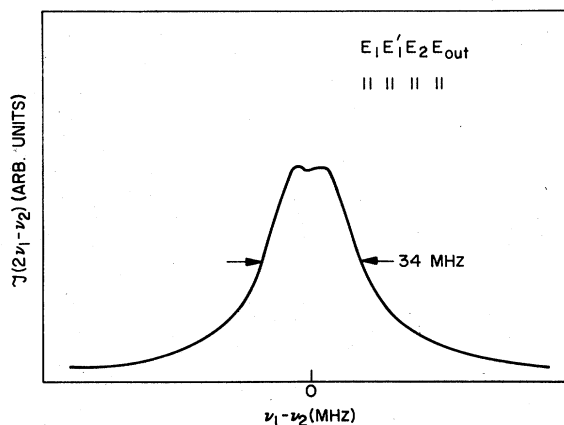


FIG. 4. Population grating resonance line shape in pure He tuned below the $^2P_{1/2}$ state ($P_{\text{He}} = 700$ Torr).

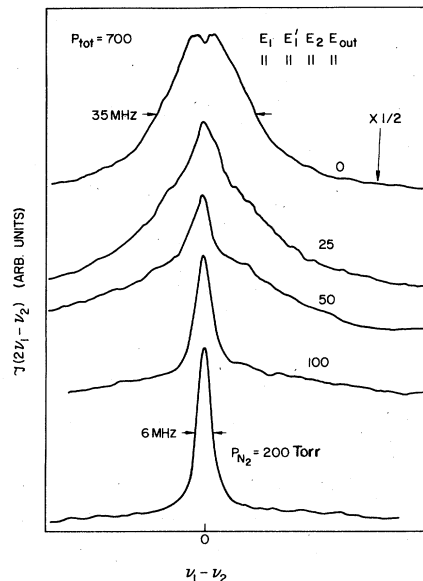


FIG. 5. Population grating resonance with lasers tuned near $^2P_{1/2}$ in the presence of excited-state quenching by N_2 . ($\Delta = 30$ GHz below $P_{1/2}$).

A typical collision-induced population grating resonance line shape at high helium pressure is shown in Fig. 4 and has FWHM of about 35 MHz and reproducible substructure. The interpretation of this line shape will be given later. To clarify the nature of the grating decay, admixtures of N_2 gas were added to the Na/He mixtures. Nitrogen quenches the P states in radiationless transitions to the 3^2S ground-state manifold by taking up the electronic energy as vibrational excitation. The results of adding nitrogen with the lasers tuned near $3P_{1/2}$ are presented in Fig. 5. The quenching broadens the resonances but also creates a residual component which has width much less than 20 MHz. This sharp feature is primarily instrumentally broadened and has the same width as coherent Raman resonances between Zeeman levels but is unaffected by the application of a magnetic field. These sharp collision-induced population grating resonances and the structure in Fig. 4 can only be understood if the strict two-level model is abandoned. More realistically, the degeneracies in the 3^2S and $3^2P_{1/2,3/2}$ manifolds of the sodium atom must be incorporated to understand the population dynamics and hence the resonance line shapes. Simple models of excited-state degeneracy, ground-state degeneracy, and sodium–inert-gas collision complex formation are worked out in the following section and used to explain the above and other results.

B. Considerations of additional degeneracy

1. Excited-state degeneracy and fine-structure changing collisions

Some previous work suggested that considering the fine-structure degeneracy in the sodium P state would alter the $(\pi T_1)^{-1} \approx 20$ MHz two-level prediction.¹² In fact, since the relaxation rates of $3^2P_{1/2}$ and $3^2P_{3/2}$ levels

are identical, collisional population exchange between these levels does not fundamentally change the relaxation rate of the grating; the excesses still refill the ground-state holes at the same rate.

Population transfer to and from nonresonant excited states is caused by fine-structure changing collisions between Na and inert buffer gases. This effect can be incor-

porated in a three-level model by adding a second excited level $|n'\rangle$ to the two-level picture. This is depicted in Fig. 2(b) where $|n\rangle$ is identified with the resonant fine-structure component and $|n'\rangle$ with levels that can only be populated and depopulated by fine-structure changing collisions. We describe this system by the following equations:

$$\begin{pmatrix} -i\delta + W_{gn} + W_{gn'} & -W_{ng} & -W_{n'g} \\ -W_{gn} & -i\delta + W_{ng} + R_{nn'} & -R_{n'n} \\ -W_{gn'} & -R_{nn'} & -i\delta + W_{n'g} + R_{n'n} \end{pmatrix} \begin{pmatrix} \rho_{gg}^{(2)} \\ \rho_{nn}^{(2)} \\ R_{n'n}^{(2)} \end{pmatrix} = \begin{pmatrix} A \\ -A \\ 0 \end{pmatrix}, \quad (7)$$

where $R_{nn'}$ and $R_{n'n}$ are fine-structure changing collision rates and A is defined as before. We let $W_{gn} + W_{ng} = W_{gn'} + W_{n'g} \equiv \Gamma$ since the P states decay spontaneously at the same rate. The resonant population modulation is

$$\rho_{nn}^{(2)} - \rho_{gg}^{(2)} = -iA \left[\frac{(R_{nn'} + 2R_{n'n}) / (R_{nn'} + R_{n'n})}{\delta + i\Gamma} + \frac{R_{nn'} / (R_{nn'} + R_{n'n})}{\delta + i(\Gamma + R_{nn'} + R_{n'n})} \right]. \quad (8)$$

Naturally when $R_{nn'} = 0$ we recover the two-level result of (4) where $\Gamma = T_1^{-1}$ of course. When fine-structure changing collisions are rapid compared to spontaneous emission (typically for $P \geq 10$ Torr), the second component of (8) broadens to become unobservable leaving a resonance with the predicted two-level width $(\pi T_1)^{-1} \approx 20$ MHz.

The intensity of the grating resonances is, however, affected by fine-structure changing collisions. The rates $R_{nn'}$ and $R_{n'n}$ are related through detailed balance by the level degeneracy ratio of $|n\rangle$ and $|n'\rangle$, $g_n/g_{n'}$, so that

$$R_{n'n} = \left[\frac{g_n}{g_{n'}} \right] R_{nn'}. \quad (9)$$

For $|n\rangle = {}^2P_{1/2}$ and $|n'\rangle = {}^2P_{3/2}$, $g_n/g_{n'} = 1/2$ and thus at $p \geq 10$ Torr, $\frac{2}{3}$ of the resonant population in (8) remains corresponding to a four-wave mixing intensity $\frac{4}{9}$ as large. When the lasers are turned near ${}^2P_{3/2}$, $\frac{5}{6}$ of the population remains resonant. The numbers $\frac{2}{3}$ and $\frac{5}{6}$ are easily interpreted physically. The $\frac{2}{3}$ ($\frac{5}{6}$) for the $P_{1/2}$ ($P_{3/2}$) state represents the half of the population modulation from the ground state ($\rho_{gg}^{(2)}$) which is unaffected by fine-structure collisions plus the fraction $g_n/(g_n + g_{n'}) = 1/3$ ($\frac{2}{3}$) of the half of the population modulation in the P state. This model by itself still does not account for the features exhibited in Figs. 4 and 5.

2. Ground-state degeneracy and optical pumping

The sharp resonances occurring with mixtures including N_2 suggest extremely long-lived gratings. These can occur when a population modulation persists because the excesses do not refill the holes from which they were formed. Relaxation of the grating, then, also depends on the relaxation rate amongst the ground states. This is determined by Na-Na spin exchange¹⁸ collisions and

under typical experimental conditions would produce homogeneous widths of less than 1 MHz, identical to those of the collision-induced coherent Raman resonances between Zeeman levels of $3S$.⁷ The long-lived population imbalance will lead to a spectrally sharp population grating resonance as long as some of the ground states contribute more strongly than others to the four-wave mixing, known from calculations to be the case.¹⁹

We model the above situation as sketched in Fig. 2(c) where two ground states $|g\rangle$ and $|g'\rangle$ are used to allow for optical pumping. The level $|g'\rangle$ is taken to be a "sink" level in the sense that it is assumed not to contribute to the population grating resonance much like the nonresonant $|n'\rangle$ levels in the case of fine-structure changing collisions. The populations of $|g\rangle$ and $|g'\rangle$ equilibrate with spin exchange rates $W_{gg'}$ and $W_{g'g}$, introducing the ground-state lifetime into the physics. Rates for the excited states to decay into the sink level, (Γ_{ng}), and to be pumped from the sink level $A' = (i/\hbar)[\mathcal{A}_{\text{coh}}, (\omega - \omega_{ng'} + i\Gamma_{ng'})^{-1}[\mathcal{A}_{\text{coh}}, \rho^{(0)}]]$ are included:

$$\begin{pmatrix} -i\delta + W_{gg'} & -W_{g'g} & -\Gamma_{ng} \\ -W_{gg'} & -i\delta + W_{g'g} & -\Gamma_{ng'} \\ 0 & 0 & -i\delta + \Gamma \end{pmatrix} \begin{pmatrix} \rho_{gg}^{(2)} \\ \rho_{g'g'}^{(2)} \\ \rho_{nn}^{(2)} \end{pmatrix} = \begin{pmatrix} A \\ A' \\ -A - A' \end{pmatrix}. \quad (10)$$

Again, the grating's frequency response exhibits two complex Lorentzian components corresponding to a biexponential relaxation of the three-level system to equilibrium

$$\rho_{nn}^{(2)} - \rho_{gg}^{(2)} = \left[\frac{-i}{\delta + i\Gamma} \right] \left[\frac{(2A + A')[\delta + i(W_{g'g} + W_{gg'})] + i(A\Gamma_{ng'} - A'\Gamma_{ng}) + i(A'W_{g'g} - AW_{gg'})}{\delta + i(W_{g'g} + W_{gg'})} \right], \quad (11)$$

where $\Gamma = \Gamma_{ng} + \Gamma_{ng'}$ is the total population decay rate of $|n\rangle$.

The expression (11) reduces to the two-level result when the last two parenthetical expressions in the numerator vanish. Each of these expressions represents an optical pumping mechanism. The condition

$$(A\Gamma_{ng'} - A'\Gamma_{ng}) \neq 0 \quad (12)$$

would mean that relaxation of atoms initially in the $|g\rangle$ state to the $|g'\rangle$ state is not balanced by the reverse process so that a net optical pumping is achieved. The condition

$$(A'W_{g'g} - AW_{gg'}) \neq 0 \quad (13)$$

describes the situation when loss mechanisms for $|g\rangle$ are different than those for $|g'\rangle$ so that population tends to pool in one or the other. For convenience we define an ef-

fective optical pumping "rate" Γ_{op} subsuming both of these mechanisms,

$$\Gamma_{op} \equiv (A\Gamma_{ng'} - A'\Gamma_{ng}) + (A'W_{g'g} - AW_{gg'}). \quad (14)$$

In the presence of either mechanism ($\Gamma_{op} \neq 0$) Eq. (11) leads to sharp features in the four-wave mixing spectra with half width given by the spin exchange rate $W_{gg'} + W_{g'g}$.

The four-wave mixing intensity varies as the squared modulus of the expression (11) leading to Lorentzian responses with ground-state and excited-state widths and a cross term which represents an interference between the scattering from ground-state and excited-state gratings over the bandwidth during which both populations can follow the intensity modulation. The resonance intensity can be written

$$\mathcal{I}(2\omega_1 - \omega_2) \propto |\chi^{(3)}|^2 \alpha \frac{4A^2}{\delta^2 + \Gamma^2} \left[\frac{\delta^2 + (W_{g'g} + W_{gg'} + \Gamma_{op})^2}{\delta^2 + (W_{g'g} + W_{gg'})^2} \right]. \quad (15)$$

Equation (15) is nearly identical to Eqs. (46) of the excellent paper by Yajima and Souma^{8(a)} which describes a somewhat different three-level system. It is also in keeping with the results of Oudar and Shen,¹¹ though written here to emphasize the interference dip in the line shape and relate it to optical pumping.

Equation (15) enables us to understand the data of Figs. 4 and 5. At high N_2 pressures, the excited-state grating is quenched by N_2 (Γ large) while optical pumping (Γ_{op}) is increased by N_2 . The residual-state grating therefore dominates and a sharp peak is observed. Optical pumping can occur in the presence of N_2 because quenching of an anisotropic distribution of $3P$ states can lead to a non-equilibrium distribution in the $3S$ ground states. At the other extreme, when no N_2 is present the excited-state grating persists for a time T_1 .

However, if there is optical pumping ($\Gamma_{op} \neq 0$), the four-wave mixing line shape can still exhibit sharp structure due to the interference between gratings cited above. In the experiments with pure He, optical pumping still occurs because one of the hyperfine components of the $3S$ state (separated by $\Omega_0 \sim 1.8$ GHz) is closer to the $3S-3P$ resonance and depleted more rapidly. One confirmation of this optical pumping mechanism is asymmetry in the line shapes of the collision-induced coherent Raman scattering resonances between different hyperfine levels of the ground state.¹² The lack of asymmetry due to optical pumping in the analogous resonances between Zeeman levels⁷ of a single hyperfine component lends support to this choice of optical pumping scheme.

When $0 < -\Gamma_{op} < W_{gg'} + W_{g'g}$, line shapes of the type seen in Fig. 4 are predicted by (15). The interference feature makes the FWHM appear broader than 20 MHz as it suppresses the line center. Experimentally, we observe that the line sharpens slightly at large detunings, presumably because the relative difference in detuning for the hyperfine levels of $3S$ is now smaller and less optical

pumping occurs. The rapid degradation of the signal strength with detuning^{1,4,5,7} prohibits a more quantitative comparison with experiment. Equation (15) can, however, reproduce the line shape of Fig. 4 quantitatively. We point out that the sign of Γ_{op} should change depending on the direction of detuning from resonance and we would expect constructive interference for tuning on the opposite sides of the $3S-3P$ resonances.

We have verified that the fundamental homogeneous broadening mechanism of the sharp resonances is caused by spin-exchange collisions which limit the ground-state lifetime. It is impractical to raise the sodium pressure high enough to observe spin exchange. The addition of Cs vapor at constant cell temperature and Na vapor pressure does not alter the propagation characteristics of the light beams, but allows the width from spin-exchange collisions to become comparable to the instrumental width (Fig. 6). Similar to analogous studies with the collision-induced Zeeman coherences,⁷ a broadening and asymmetry in this sharp resonance appear in the presence of cesium.

An extremely interesting and instructive analog to the phenomena discussed above occurs in the resonant phase conjugation experiments of Lam, Steel, and McFarlane.¹⁰ There, only sodium is present and the lasers are tuned to the $3S(F=2) \rightarrow 3P_{3/2}(F=3)$ transition of sodium where no optical pumping occurs. A degenerate frequency population grating resonance occurs without collisional dephasing when tuned within the inhomogeneous profile of the resonance. The resonance is Doppler free because a particular velocity group $v=0$ is selected by the lasers, and its homogeneous FWHM is found to be 20 MHz in accord with the two-level theory. Adding two Torr of inert buffer gas (Ne) leads to a resonance of about 5 MHz width^{10(c)} and this is explained by these authors in terms of velocity changing collisions between sodium and the inert gas. In the language of this paper, the ground-state holes are not filled properly because collisions remove

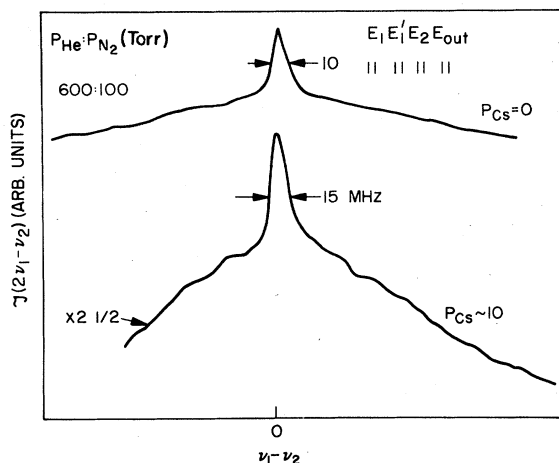


FIG. 6. Effect of cesium admixture on sharp population grating resonance.

atoms from the resonant velocity group. This destroys the excited-state grating just as do fine-structure changing collisions in our experiments and results in a ground-state velocity distribution imbalance and therefore a ground-state grating until the population rethermalizes much like our S sink states. In their experiments, destruction of the ground-state grating is much slower than that of the excited-state grating due to higher velocity-changing collision cross sections for the excited states, and their 5 MHz ground-state grating widths are also determined by laser frequency jitter limitations. In our case, destruction of the excited-state grating by collisional quenching is much faster than the rate at which the ground-state grating is destroyed when the quenching mechanism leads to a net optical pumping of the ground state.

3. Molecular formation and dissociation

The onset of collisional narrowing of the Doppler width occurs at very low pressures in xenon buffer gas because of its large mass which makes for efficient velocity changing collisions. In sodium with 100 Torr of pure Xe, we find that, for an alignment angle of about 2 deg, the linewidth of the population grating resonance is less than 20 MHz (Fig. 7), and is the same as the width of the Zeeman resonances in Xe at that pressure. This resonance is unaffected by an external magnetic field and its width is unchanged by the addition of N_2 . Evidently, the addition of Xe leads to a quite strong ground-state grating, much stronger than those in N_2 . At lower pressures (< 60 Torr Xe), line wings corresponding to the excited-state grating can be observed (Fig. 8) but these are apparently broadened away by the addition of xenon.

The mechanism we propose to explain these data is excimer formation of $NaXe$ in an excited π^* state when 2P sodium atoms collide with ground-state Xe atoms. This affects the excited-state grating in much the same way as irreversible fine-structure changing collisions would; molecular formation serves to remove the P state atoms from resonance. The net result is to leave a resonant

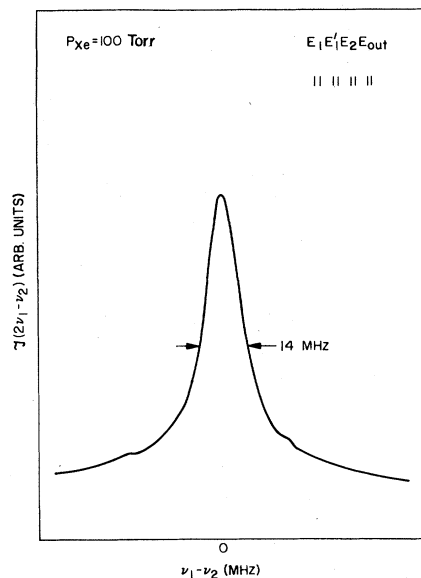


FIG. 7. Population grating resonance in 100 Torr Xe ($\Delta = 20$ GHz below $P_{1/2}$).

ground-state grating, periodic unfilled holes in the ground state. A model calculation of such an effect [Fig. 2(a)] corroborates this qualitative reasoning. As with the case of ground-state sinks, the addition of an extra state to the two-level model decouples excited- and ground-state population evolutions and introduces the ground-state lifetime into the physics.

Excimer formation between $Na(4^2S)$ and Ar, Kr, and Xe has been observed²⁰ and even ground-state "sticking collisions" between Rb and Ar, Kr, and Xe have been reported.^{21,22} In the latter case, lifetimes of the order of 10 ns were associated with these complexes formed in biatomic collisions. Generally, since energy and momentum cannot be conserved in a two-body reaction, three-body collisions are required for stable molecular formation. In the instances cited above, the long relaxation time "re-

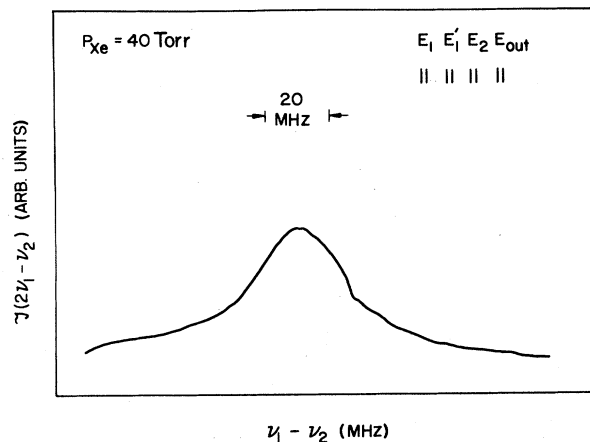


FIG. 8. Population grating resonance in 40 Torr Xe ($\Delta = 20$ GHz below $P_{1/2}$).

flects the presence of metastable states associated with resonances in (interatomic) scattering^{21(b)} which can occur whenever the relative kinetic energy of colliding atoms equals the energy of a bound state of the complex. Other authors²³ report significant formation of Na(²P)-Ar complexes in three-body collisions at only 60 Torr of Ar pressure and this, too, could be an important contributing factor in the destruction of the excited-state grating.²⁴

In the experiments of Bouchiat *et al.*,²¹ the Rb-Kr complexes formed were found to be dissociated by collisions with helium. Adding helium to the 100 Torr of Xe modifies the spectrum of Fig. 7 as shown in Fig. 9. Indeed, helium collisions appear to restore the excited-state grating, presumably by dissociating the metastable Na-Xe excimers. We note that the spectrum at 600 Torr He and 100 Torr Xe very much resembles the four-wave mixing spectrum in pure He.

The above studies are well explained by the model of Fig. 2(d). We assume that Na(3P)-Xe collisions form metastable complexes $|M\rangle$ which remove 3P atoms from resonance with rate R_{nM} and that collisions can also result in dissociation of $|M\rangle$ to its original constituents with rate R_{Mn} . The equations are those of

$$\begin{pmatrix} -i\delta + W_{gg'} + W_{g'g} & -\Gamma & 0 \\ 0 & -i\delta + \Gamma + R_{nM} & -R_{Mn} \\ 0 & -R_{nM} & -i\delta + R_{Mn} \end{pmatrix} \begin{pmatrix} \rho_{gg}^{(2)} \\ \rho_{nn}^{(2)} \\ \rho_{MM}^{(2)} \end{pmatrix} = \begin{pmatrix} A \\ -A \\ 0 \end{pmatrix}, \quad (16)$$

where an effective ground-state width $W_{gg'} + W_{g'g}$ has been retained from the calculation of the preceding section.

The second ground state is not considered explicitly so that (16) can be solved analytically. The roots of the characteristic polynomial $P(\delta)$ associated with the above matrix represent Lorentzian half-widths which should be observed in the spectra. Here,

$$P(\delta) = (-i\delta + W_{gg'} + W_{g'g})[-\delta^2 - i\delta(\Gamma + R_{nM} + R_{Mn}) + \Gamma R_{Mn}]. \quad (17)$$

The characteristic full widths are

$$2|\delta_{1/2}| = 2(W_{gg'} + W_{g'g}), \quad (18a)$$

$$2|\delta_{1/2}| = \Gamma + R_{nM} + R_{Mn} + [(\Gamma + R_{nM} + R_{Mn})^2 - 4\Gamma R_{Mn}]^{1/2}, \quad (18b)$$

$$2|\delta_{1/2}| = \Gamma + R_{nM} + R_{Mn} - [(\Gamma + R_{nM} + R_{Mn})^2 - 4\Gamma R_{Mn}]^{1/2}. \quad (18c)$$

The first root represents the ground-state width which is manifest when formation of $|M\rangle$ irreversible on the experimental timescale prevents the ground-state holes from filling. We examine the last two roots in the limiting cases of dominant complex formation ($R_{nM} \gg \Gamma, R_{Mn}$) and rapid dissociation ($R_{Mn} \gg \Gamma, R_{nM}$). With rapid complex formation the widths describing the excited-state grating reduce to a strong root with

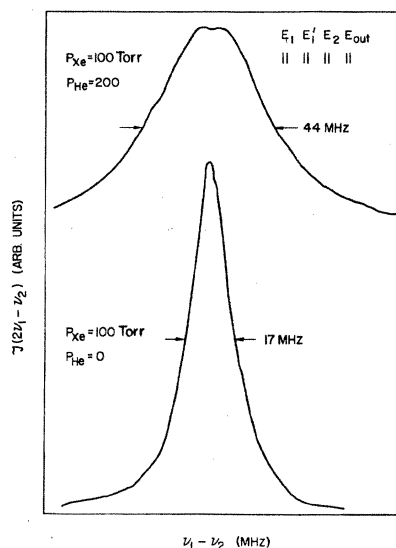


FIG. 9. Typical population grating resonances in Xe/He mixtures. ($\Delta = 20$ GHz below $P_{1/2}$).

$$2|\delta_{1/2}| = \Gamma + R_{nM} \quad (19)$$

and much weaker process of width

$$2|\delta_{1/2}| = R_{Mn}. \quad (20)$$

When rapid dissociation dominates complex formation, the roots become

$$2|\delta_{1/2}| = \Gamma,$$

$$2|\delta_{1/2}| = \Gamma + R_{nM} + R_{Mn}.$$

We note that this latter case has the same roots as the case of fine-structure changing collisions where $|M\rangle$ is identified with $|n'\rangle$. The essential difference between these cases, that $|M\rangle$ does not decay directly to $|g\rangle$, had been made negligible by rapid destruction of $|M\rangle$ to reform $|n\rangle$ which can decay to $|g\rangle$ and refill the ground-state holes. For large dissociation rates, then, the amplitude but not the linewidth associated with the excited-state grating is affected by complex formation of excited sodium with xenon. This is just as in the fine-structure changing collision case and the spectrum also reverts to the simple case of Sec. I.

The results of population grating resonance studies in argon buffer gas appear qualitatively similar to those in xenon but are considerably less clear cut because the collisional narrowing of the Doppler width in argon is much slower. We note that Ewart *et al.*²³ have reported excimer formation between the 3^2P state of sodium and ground-state argon.

A possible alternative mechanism for creating a ground-state grating is along the lines of the optical pumping mechanism suggested for collisional quenching by N_2 . The NaXe excimers could fall apart in such a way as to leave the ground state of sodium in a highly non-equilibrium population distribution. The strength of the grating resonance may be an indication that this mechanism is less likely.

IV. INTERFERENCE BETWEEN ZEEMAN AND POPULATION GRATING RESONANCES

Thus far we have presented results of experiments with incident field polarizations \vec{E}_1 and \vec{E}'_1 parallel to \vec{E}_2 . The selection rules require $\Delta m_F = 0$ between the initial and final state in the 3^2S manifold, and the four-wave mixing output, \vec{E}_{out} , is parallel to the input fields. When \vec{E}_1 and \vec{E}'_1 are perpendicular to \vec{E}_2 then $\Delta m_F = \pm 1$ resonances are selected.⁷ Population gratings are excluded and the four-wave mixing output results from Raman-type coherences between Zeeman sublevels of $3S$. The resonance positions are sensitive to external magnetic fields and the homogeneous widths are characterized by sodium-sodium spin-exchange collision rates.

Interference between different $\chi^{(3)}$ processes has been demonstrated previously,²⁵ and used to measure relative cross sections for coherent Raman scattering and two-photon absorption. An interesting example of this phenomenon occurs when both Zeeman and population grating resonances are allowed by the polarization configuration. We consider here a simple example of interference where $\vec{E}(\omega_1)$ and $\vec{E}'(\omega_1)$ are parallel polarized and $\vec{E}(\omega_2)$ is linearly polarized at an arbitrary angle ϕ with respect to them. Call the direction of $\vec{E}(\omega_1)$ the \hat{z} direction and let the orthogonal direction in the plane of the fields be \hat{x} as illustrated in Fig. 10. In the absence of \vec{B} , we can think of the component of $\vec{E}(\omega_2)$ parallel to $\vec{E}(\omega_1)$ creating a population modulation and the perpendicular component creating a Zeeman coherence. The coherent emissions corresponding to these processes will have orthogonal polarizations and what is observed will depend upon the angle ψ of our output polarizer in the plane of the fields. At angles ψ other than $0, \pi/2, \pi,$ and $3\pi/2$ both processes (i.e., both sets of radiating antennae) contribute to the total output field and the radiated fields will interfere. The observed field will be

$$E_{out}(\psi)\alpha P_z \sin\psi + P_p \cos\psi, \quad (21)$$

where P_z and P_p are nonlinear electric polarizations corresponding to the Zeeman and population coherences and are given by

$$P_z = \chi_z^{(3)} E_1 E'_1 E_2^* \sin\phi, \quad (22)$$

$$P_p = \chi_p^{(3)} E_1 E'_1 E_2^* \cos\phi. \quad (23)$$

The resulting four-wave mixing intensity will be

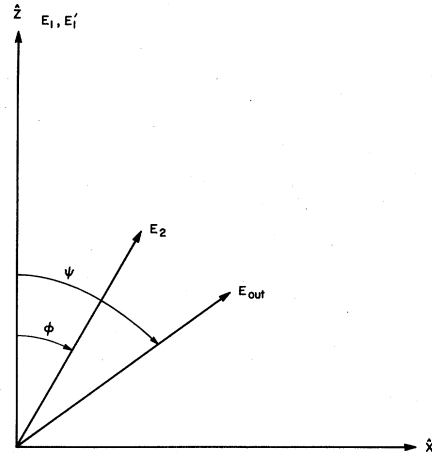


FIG. 10. Schematic of polarization scheme for interference experiments.

$$\mathcal{I}_{out} \propto |E_{out}(\psi)|^2 \alpha |P_z|^2 \sin^2\psi + |P_p|^2 \cos^2\psi + (P_z^* P_p + P_p^* P_z) \sin\psi \cos\psi, \quad (24)$$

where the last term is an interference term which can cancel the output entirely when $P_z = \pm P_p$ and $\psi = \pi/4, 3\pi/4$.

Figure 11 shows data from the more general case described above with $\phi = 20^\circ$ and ψ varied to demonstrate the nature of this interference effect. Both constructive and destructive interferences between collision-induced Zeeman and population grating resonances in pure helium are observed as the output analyzer is rotated. The bandwidth of the interference structure is characteristic of the width of the Zeeman resonances. We are also able to verify that this effect is distinct from the interference dip due to an optically pumped ground-state grating by applying a magnetic field in the \hat{z} direction [Fig. 11(d)]. In an external field (along \hat{z} in the experiment) the interference features due to Zeeman coherences are removed from $\omega_1 - \omega_2 = 0$ leaving only the ground-state grating dip at $\omega_1 - \omega_2 = 0$ which is much weaker.

A more detailed attempt at modeling the line shapes of Figs. 11(a)–11(c) runs into fundamental difficulties. Expressions for the polarizations P_z and P_p where the denominators resonant in the difference frequency are written explicitly are given by

$$P_z = \frac{C_z \sin\psi}{\delta + i\Gamma_z} \quad (25)$$

and

$$P_p = \frac{C_p \cos\psi}{\delta + i\Gamma_p}. \quad (26)$$

In the extreme narrowing limit where the velocity distribution is Lorentzian,^{15,26} these expressions are correctly averaged over the velocity distribution if we take the damping widths Γ_z and Γ_p to be the sum of appropriate homogeneous and residual Doppler widths.¹⁹ In practice, Γ_p is primarily homogeneous width and Γ_z inhomogene-

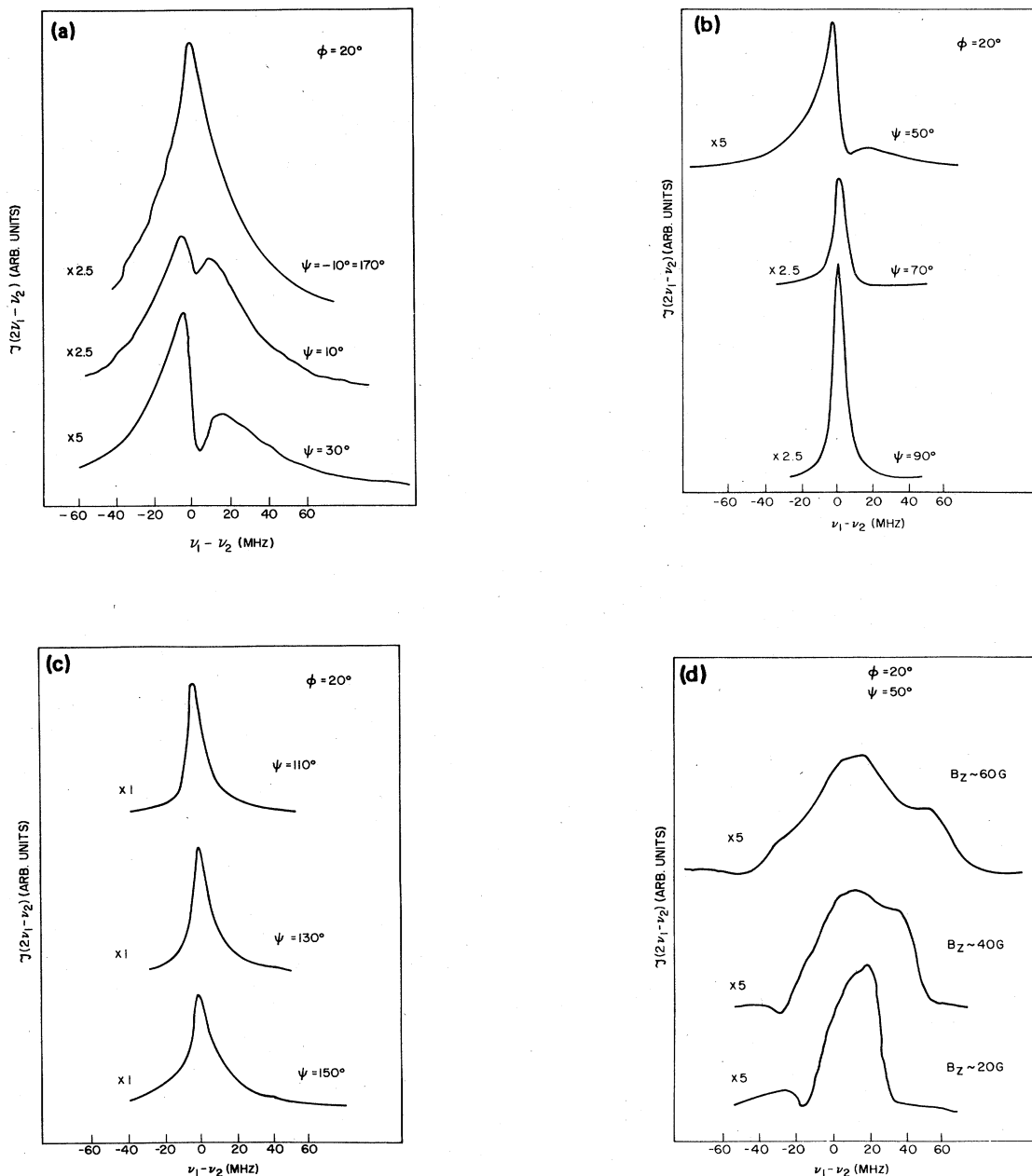


FIG. 11. (a)–(c) Interference between Zeeman and population grating resonances; (d) interference between Zeeman and population grating resonances in an external magnetic field along z .

ous. The instrumental width is smaller than either of these. The constants C_z and C_p contain identical resonant denominators and identical field terms $E_1 E_1^* E_2^*$, and dipole matrix element products which are all real. The constants C_z and C_p are therefore complex numbers in phase or 180° out of phase and we can assume them to be real

without loss of generality. Physically, it is not a surprising result that identical fields would drive these sets of antennae either in phase or 180° out of phase save for the resonant denominators' damping which we have removed explicitly in (25) and (26). Equation (24) can then be recast as

$$\mathcal{F}_{\text{out}}(\phi, \psi) = \frac{(C_z \sin \psi + C_p \cos \psi)^2 \delta^2 + (\Gamma_p C_z \sin \psi + \Gamma_z C_p \cos \psi)^2}{(\delta^2 + \Gamma_z^2)(\delta^2 + \Gamma_p^2)} \quad (27)$$

which is symmetric in $\delta = \omega_1 - \omega_2$. The line shapes of Figs. 11 are distinctly asymmetric and this is not yet completely understood.

V. SUMMARY AND CONCLUSIONS

We have reported results of high-resolution studies of near degenerate collision-induced four-wave light mixing in sodium vapor with inert buffer gases. High resolution experiments enable us to understand inhomogeneous and homogeneous broadening mechanisms for population grating resonances in four-wave mixing. The results are explained qualitatively in terms of a grating picture and modeled quantitatively using time dependent perturbation theory in the presence of damping.

At low pressures of buffer gas the residual Doppler width contributes significantly to the linewidth but at higher pressures velocity changing collisions reduce this width by preserving the spatial modulation of the excited sodium density. More importantly, collisional narrowing of the residual Doppler width makes it feasible to study the homogeneous broadening mechanisms unencumbered.

The data show that a detailed treatment of the degeneracy of the sodium atoms is necessary to understand the four-wave mixing line shapes and intensities. Excited-state fine-structure degeneracy allows fine-structure changing collisions to introduce a second component (broad at pressures ≥ 10 Torr) to the two-level line shape and reduce the intensity of the two-level grating. The width of the remaining component is unaltered because the fine-structure components decay to refill the ground state at the same rate.

The four-wave mixing resonance broadens when the excited-state grating is collisionally quenched by N_2 and leaves a sharp component. This sharp resonance is attributable to a residual ground-state grating from a collision-induced optical pumping and has width characteristic of the ground-state lifetime. Even in the absence of N_2 , optical pumping occurs because the different hyperfine components of the ground state are detuned by different amounts from the $3S-3P$ resonance. In this case interference between ground-state and excited-state grat-

ings can explain the anomalously large linewidth and the structure in the line shape. In xenon buffer gas, sharp ground-state population gratings were also observed. There, the excited-state quenching mechanism is probably excimer formation between the highly polarizable Xe atoms and the sodium P states.

Results of experiments demonstrating interference between the collision-induced population grating resonances and collision-induced coherent Raman resonances between ground-state Zeeman levels are also presented. From these, one can deduce relative intensities and phases of the corresponding electric polarizations and a dephasing between the susceptibilities for these processes which is not yet understood has been documented. The collision-induced resonances arise because collisions remove the destructive interference between different time-ordered quantum-mechanical amplitudes contributing to $\chi^{(3)}$. The analogous dephasing between different intermediate state ordered pathways contribution to $\chi^{(3)}$ could explain this phenomena but further work needs to be done to clarify this speculation.

The experimental observation and characterization of damping-induced nonlinear phenomena has stimulated theoretical work³⁻⁵ as well as applications to other scientific problems. Dephasing-induced four-wave mixing experiments have been used to study relaxation times in organic dyes in solution⁸ and used to do novel spectroscopy of excited-state vibrations in molecular crystals.²⁷ Atomic collisional potentials²⁸ and properties of velocity changing collisions¹⁷ have been explored by pressure-induced four-wave mixing experiments. In conclusion, dephasing-induced coherent phenomena are promising research tools to study collisional properties, population dynamics and chemical interactions.

ACKNOWLEDGMENTS

Helpful discussions with Professor Tom Mossberg, Professor Paul Berman, and Dr. Juan Lam are gratefully acknowledged. This work was supported by the U. S. Joint Services Electronics Program under Contract No. 00014-75-C-0648.

*Present address: AT&T Bell Laboratories, 600 Mountain Avenue, Murray Hill, NJ 07974.

¹N. Bloembergen, A. R. Bogdan, and M. C. Downer in *Laser Spectroscopy V*, edited by A. R. W. McKellar, T. Oka, and B. P. Stoicheff (Springer, Heidelberg, 1981), p. 157.

²N. Bloembergen, H. Lotem, and R. T. Lynch, Jr., *Indian Pure and Appl. Phys.* **16**, 151 (1978).

³(a) S. Y. Yee, T. K. Gustafson, S. A. J. Druet, and J-P. E. Taran, *Opt. Commun.* **23**, 1 (1977); (b) T. K. Yee and T. K. Gustafson, *Phys. Rev. A* **18**, 1597 (1978); (c) J. G. Fujimoto and T. K. Yee, *IEEE J. Quantum Electron.* **19**, 861 (1983).

⁴(a) G. Grynberg, in *Laser Spectroscopy V*, edited by A. R. W. McKellar, T. Oka, and B. P. Stoicheff (Springer, Heidelberg, 1981); (b) *J. Phys. B* **14**, 2089 (1981); (c) *Opt. Commun.* **38**, 439 (1981).

⁵V. Mizrahi, Y. Prior, and S. Mukamel, *Opt. Lett.* **8**, 145

(1983).

⁶(a) N. Bloembergen and Y. R. Shen, *Phys. Rev.* **133**, A37 (1964); (b) N. Bloembergen, *Nonlinear Optics* (Benjamin, New York, 1965).

⁷L. J. Rothberg and N. Bloembergen, *Phys. Rev. A* **30**, 820 (1984).

⁸(a) T. Yajima and H. Souma, *Phys. Rev. A* **17**, 309 (1978); (b) T. Yajima, H. Souma, and Y. Ishida, *Phys. Rev. A* **17**, 324 (1978).

⁹(a) D. G. Steel, R. C. Lind, J. F. Lam, and C. R. Giuliano, *Appl. Phys. Lett.* **35**, 376 (1979); (b) D. G. Steel, J. F. Lam, and R. A. McFarlane, in *Laser Spectroscopy V*, edited by A. R. W. McKellar, T. Oka, and B. P. Stoicheff (Springer, Heidelberg, 1981); (c) J. F. Lam, D. G. Steel, and R. A. McFarlane, *Phys. Rev. Lett.* **49**, 1628 (1982); (d) J. F. Lam and R. L. Abrams, *Phys. Rev. A* **26**, 1539 (1982).

- ¹⁰See, e.g., J. R. Salcedo, A. E. Siegman, D. D. Dlott, and M. D. Fayer, *Phys. Rev. Lett.* **41**, 131 (1978).
- ¹¹J.-L. Oudar and Y. R. Shen, *Phys. Rev. A* **22**, 1141 (1980).
- ¹²A. R. Bogdan, M. W. Downer, and N. Bloembergen, *Opt. Lett.* **6**, 348 (1981).
- ¹³(a) A. C. Eckbreth, *Appl. Phys. Lett.* **32**, 421 (1978); (b) S. Chandra, A. Compaan, and E. Wiener-Avneer, *Appl. Phys. Lett.* **33**, 867 (1978); (c) Y. Prior, *Appl. Opt.* **19**, 1741 (1980).
- ¹⁴See, e.g., J. Nilssen and A. Yariv, *J. Opt. Soc. Am.* **71**, 180 (1981).
- ¹⁵R. H. Dicke, *Phys. Rev.* **89**, 472 (1953).
- ¹⁶P. Wittke and R. H. Dicke, *Phys. Rev.* **103**, 103 (1956); **103**, 620 (1956).
- ¹⁷L. J. Rothberg and N. Bloembergen, in *Proceedings of the International Conference on Lasers '83* (Society for Optical and Quantum Electronics, McLean, Virginia, in press).
- ¹⁸W. Happer, *Rev. Mod. Phys.* **44**, 169 (1972).
- ¹⁹L. J. Rothberg, Ph.D. thesis, Harvard University, 1984 (unpublished).
- ²⁰(a) A. Tam, G. Moe, W. Park, and W. Happer, *Phys. Rev. Lett.* **35**, 85 (1975); (b) A. C. Tam, G. Moe, B. R. Bulos, and W. Happer, *Opt. Commun.* **16**, 376 (1976).
- ²¹(a) M. Aymer, M. A. Bouchiat, and J. Brosset, *Phys. Lett.* **24A**, 753 (1967); (b) M. A. Bouchiat, J. Brosset, and L. Pottier, *Phys. Rev. Lett.* **19**, 817 (1967); (c) C. C. Bouchiat, M. A. Bouchiat, and L. C. L. Pottier, *Phys. Rev.* **181**, 144 (1969); (d) C. C. Bouchiat and M. A. Bouchiat, *Phys. Rev. A* **2**, 1274 (1970).
- ²²F. Hartmann and F. Hartmann-Bourton, *Phys. Rev. A* **2**, 1885 (1970).
- ²³(a) P. Ewart, A. I. Ferguson, and S. V. O'Leary, *Opt. Commun.* **40**, 147 (1981); (b) P. Ewart and S. O'Leary, *J. Phys. B* **15**, 3669 (1982).
- ²⁴A great deal of work on alkali-metal-rare-gas complexes not mentioned here has been done. The references cited here are specified to the systems of interest and are meant to lend plausibility to the qualitative explanation of our data we have put forth.
- ²⁵(a) M. D. Levenson and N. Bloembergen, *Phys. Rev. B* **10**, 4447 (1974); (b) H. Lotem, R. T. Lynch, and N. Bloembergen, *Phys. Rev. A* **14**, 1748 (1976).
- ²⁶S. G. Rautian and I. I. Sobel'man, *Usp. Fiz. Nauk* **90**, 209 (1966) [*Sov. Phys.—Usp.* **9**, 201 (1967)].
- ²⁷(a) J. R. Andrews and R. M. Hochstrasser, *Chem. Phys. Lett.* **82**, 381 (1981); (b) **83**, 427 (1981); (c) J. R. Andrews, R. M. Hochstrasser, and H. P. Trommsdorff, *Chem. Phys.* **62**, 87 (1981).
- ²⁸(a) R. Scholz, J. Mlynek, A. Gierulski, and W. Lange, *Appl. Phys. B* **28**, 191 (1982); (b) R. Scholz, J. Mlynek, and W. Lange, in *Laser Spectroscopy VI*, Proceedings of the Sixth International Conference on Laser Spectroscopy, edited by H. P. Weber and W. Luthy (Springer, Heidelberg, 1983); (c) R. Scholz, J. Mlynek, and W. Lange, *Phys. Rev. Lett.* **51**, 1761 (1983).